RESEARCH PAPER

Fatigue and failure behaviour of friction welded steel joints under normal and shear stresses

IIW Document XIII-2944-2022, German Delegation

Jörg Baumgartner[1] · Lorenz Uhlenberg[2] · Frank Trommer[3] · Ann-Christin Hesse[2] · Markus Köhler[2] · Klaus Dilger[2]

Abstract
Rotary friction welding is a fast and efficient joining process with the possibility to join materials that are not weldable by conventional GMAW-processes. If done properly, the welds have a static and fatigue strength higher than the base material. However, in literature, there exists only sparse information on the design and assessment of these joints in terms of fatigue. The fatigue strength of two material combinations, S355-S355 and S355-1.4301, is investigated based on two specimen conditions, (1) with flash and (2) with flash mechanically removed. In the majority of tests, failure occurred outside the weld zone, in the base material. The derived endurable nominal stresses are compared to the design S-N curve of conventionally welded specimens and show a more than 50% higher fatigue strength.

✉ Jörg Baumgartner
  joerg.baumgartner@lbf.fraunhofer.de

  Lorenz Uhlenberg
  l.uhlenberg@tu-braunschweig.de

  Frank Trommer
  frank.trommer@h2.de

  Ann-Christin Hesse
  a.hesse@tu-braunschweig.de

  Markus Köhler
  markus.koehler@tu-braunschweig.de

  Klaus Dilger
  k.dilger@tu-braunschweig.de

[1] Fraunhofer LBF, Bartningstr. 47, Darmstadt 64289, Germany

[2] Institute of Joining and Welding, Technische Universität Braunschweig, Langer Kamp 8, Braunschweig 38106, Germany

[3] Institute of Mechanical Engineering, Hochschule Magdeburg-Stendal, Breitscheidstraße 2, Magdeburg 39114, Germany

1 Introduction

1.1 Friction welding

Friction welding belongs to the group of pressure welding processes. The energy required for the weld in the form of heat is generated by the relative movement of the components under pressure. Depending on the type of relative movement, a distinction is made between rotary, linear, orbital and friction welding with angular oscillation [1, 2], with rotary friction welding being the standard process. In order to achieve certain properties of the friction welded joint, the relative speed and axial pressure must be adjusted depending on the base materials and the process phase. The main parameters of the friction welding process are the rotational speed, the axial force and optionally the control of the process via time or the axial feed.

The parameter settings are assigned to different process phases (Fig. 1). In the contact phase, one of the workpieces is set in rotation and the parts to be joined are brought into contact with a low axial force. Mechanical roughness removal and plastic deformation smooth the faying surfaces and increase the joining cross-section. The main heat gener-

ation takes place in the friction phase. The increased axial force and simultaneous rotation lead to the generation of frictional heat. The constant heat input into the workpieces causes the temperature in the joining zone to rise and leads to a softening of the material. Due to the acting axial force, highly plasticized material is displaced to the outside and forms the weld flash. When a sufficient amount of heat has been generated, spindle rotation is stopped and the forging and holding phase is initiated. The forge force is applied when the spindle is completely stopped or already during the braking phase. The amount of forge force depends on the shape and size of the joining surfaces and the base material of the parts. It ensures a constant contact pressure during component cooling so that diffusion and recrystallization processes can take place.

Friction welding is used in almost all areas of manufacturing [3–6]. It is preferred when the highest joint qualities and a robust and repeatable process are required. In addition, a wide range of materials and material combinations can be friction welded, which are difficult or impossible to join using other welding processes [7–11]. Unlike fusion welding processes, the joining temperature is below the melting temperature [12], which is why many metallurgical problems hardly play a role in friction welding. For example, the coarse grain structure typical of fusion welding is absent, and the occurrence of undesirable microstructural phases is greatly reduced. In contrast, a very fine-grained and pore-free microstructure is formed, which achieves a high static strength, in some cases higher than the base metal.

During the welding process, a typical geometry with a welding flash is created due to the process (Fig. 2). Geometrically, there exist two types of geometrical notches: first, the flash base notch between flash and the parent material, and second, the flash fork notch in case of a bifurcated flash.
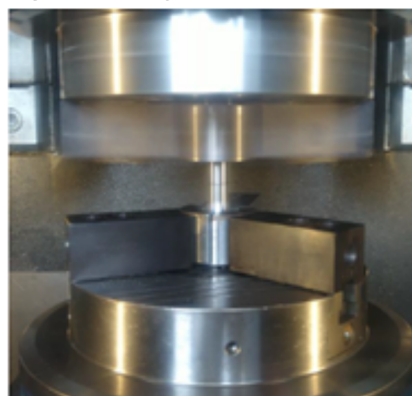
Three types of micro-structures can be differentiated [13]: the one in the parent resp. base material, the one in the heat affected zone where the material is heat treated but not deformed, and the thermo-mechanically heated zone in which the material experiences heat combined with plastic deformation. The latter zone includes a so-called weld centre zone close to the interface which exhibits a different microstructure due to extreme plastic deformations.

a) contact phase

b) friction phase

c) forging phase / holding

Fig. 1 Rotary friction welding process phases

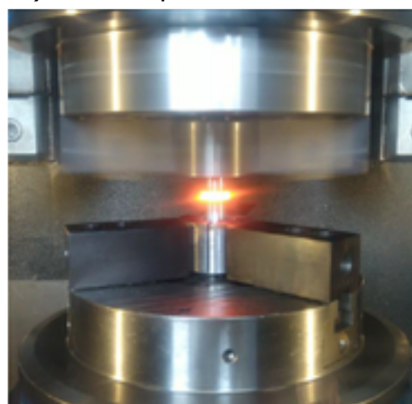## 1.2 Fatigue and assessment approaches

1.2.1 Fatigue behaviour

Welded joints and structures joined by conventional welding processes, such as arc or beam welding, show a comparatively low fatigue strength in the as-welded condition. The reason behind this are sharp notches at the transition between weld metal and heat affected zone that are induced by these processes. These notches lead to a high stress concent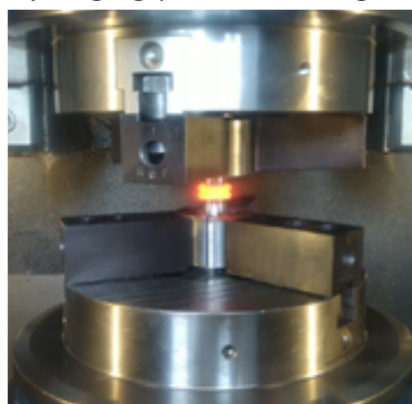ration and, subsequently, to high local stresses. During cyclic loading, cracks initiate quite early compared to the total fatigue life. The fatigue life is dominated by crack propagation.

In case of a post-weld treatment, such as burr grinding or TIG-dressing, the fatigue-critical notches at the weld toes are removed or largely rounded. This leads to a strong reduction of the stress concentration and to a highly improved fatigue strength.

1.2.2 Fatigue assessment of welded joints

For the fatigue assessment of welded joints, various approaches are available [14]. In industrial practice, linear-elastic and easily applicable approaches, such as the nominal, the structural or the notch stress approach, are used. The endurable stresses for all approaches are derived and defined for joints in as-welded condition that possess small weld toe and weld root radii with a high stress concentration.

These sharp radii lead to the characteristic fatigue behaviour [15]: Crack initiation starts early, and the total fatigue life is dominated by crack propagation. This leads to S-N curves with a steep slope of $k = 3$ [16]. The knee point is positioned typically in the range of $10^6 \leq N_k \leq 10^7$ cycles.

1.2.3 Fatigue assessment of wrought materials

For non-welded components made from steel, aluminium alloys or cast iron, the Mechanical Engineering Research Federation (FKM) provides a guideline [17] for the static strength assessment and for the fatigue assessment. The approach for the static and fatigue assessment is primarily based on the ultimate strength as the main influencing factor of the material. From this, an endurable stress amplitude is derived. In any case, the slope of the S-N curve k and the cycles at the knee point N_k are kept constant at $k = 5$ and $N_k = 10^6$.

The influence of stress gradients, surface roughness, temperature of mean stresses and others is assessed by factors that increase or decrease the endurable stresses at the knee point. These factors depend also on the material, i.e. the material strength and the material group.

1.3 Fatigue of friction welded joints

Friction welded joints in the as-welded state are characterized by two types of notches. First is the notch between base metal and flash (Fig. 2). The stress concentration of the notch is defined by the curvature resp. the radius in this area. In case of a bifurcated fork, a second notch is located between the flash "tongues" coming from both metals. In case of a non-properly welded joint, notches at non-connected areas in the interface might be present. All these notches are potential locations of fatigue crack initiation.

In many industrial applications, the flash and with it the geometrical notches are mechanically removed. In this case, different potential failure regions emerge: Zones with the lowest endurable stresses can be the base material or the metallurgical notch in the interface.

In literature, few investigations on the fatigue strength of rotary friction welded joints are available:

Hasegawa [18] investigated the influence of different welding parameters on the fatigue strength. Overall, four steels with different carbon contents have been used. In addition, the upset pressure was varied. Failure occurred at the flash base notch. The results showed an increase in fatigue strength with increasing material strength. In addition, an increase in fatigue strength was identified with decreasing contact pressure. The reason behind this are larger radii of the flash base notch and subsequently a decrease in stress concentration factor.

Paventhan [19] performed fatigue tests on dissimilar specimens made from medium carbon steel and austenitic stainless steel with flash removed. The failure occurred in the interface. The dissimilar welded joints showed lower endurable loads compared to both base materials.

Neumann and Schober [20] evaluated various test series and recommended quality classes and dedicated FAT-classes for the nominal stress approach in close agreement to the IIW-recommendations [16]. For welded similar materials, low residual stresses should be assumed, and for dissimilar materials, high tensile stresses. In contrast, in [12], both authors recommend an assessment based on the algorithm from the TGL-recommendation, given by the former German Democratic Republic [21].

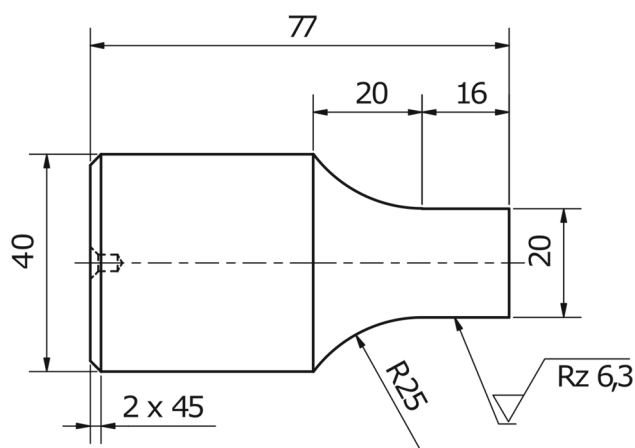**Fig. 2** Geometry and microstructural zones of a rotary friction weld
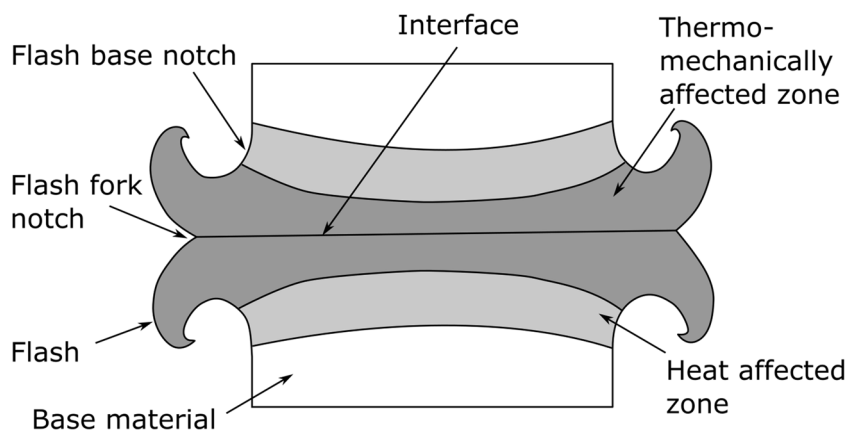
Fig. 3 Geometry of the shafts used for friction welding

Fig. 4 Machine setup for welding the specimens

2 Manufacturing

2.1 Materials and geometry

The tests are divided into two test series. For test series 1, identical round bars made of the structural steel S355J2 (1.0570) are used. In test series 2, a material combination of S355J2 is welded to the stainless austenitic steel X5CrNi18-10 (1.4301).

The specimen geometries are identical for all tests (Fig. 3). The shafts used for welding have a diameter in the clamping region of $D_a = 40$ mm that is reduced to $D_i = 20$ mm in the region of welding. The total length of a single round bar is 77 mm.

2.2 Machine setup and welding parameters

The friction welding is carried out on a CNC-controlled friction welding machine (Fig. 4). The axial force is applied servo-electrically with a maximum force of $F_{max} = 200$ kN. The occurring process forces are recorded via an integrated force measurement platform and used as a control variable.

As usual in friction welding, a force-controlled process is conducted. The friction phase is additionally displacement-controlled, while the forge and holding phases are time-controlled. Table 1 shows the process parameters used for welding series 1 (S355-S355) and welding series 2 (S355-1.4301). Figure 5 shows an example of a process diagram

from welding series 1. The friction time lasts here for about $t = 6.5$ s.

The welding processes for both series were very stable and showed no abnormalities in the process curves. This is also confirmed by the only slight variation in total shortening with a standard deviation of 0.061 mm and provides an excellent basis for further investigations.

After welding, the flash of 50% of the specimens was removed by turning. The net diameter of these specimens was set to $D_i = 18$ mm or $D_i = 16$ mm. After turning, the surface roughness was $R_z = 6.3$ μm and thus identical to the roughness of the shafts used for welding.

The specimens made from S355-S355 have been heat treated at 550 °C $\leq T \leq$ 600 °C for 120 Minutes in order to relieve residual stresses from the manufacturing process. A stress relief annealing of the specimens made from S355-1.4301 was not carried out in order to avoid the formation of chromium carbides that could have a negative effect on the fatigue strength.

3 Characterization

3.1 Residual stress

Residual stress measurements were carried out for both material combinations by X-ray diffraction using the $\sin^2 \psi$

Table 1 Process parameters of friction welding

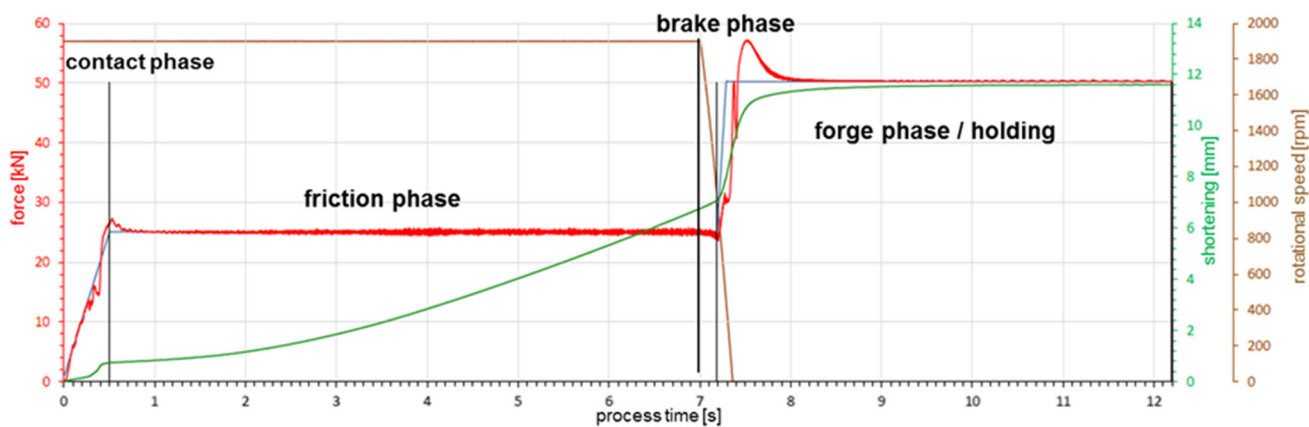| Series	Set-up time contact (s)	Friction force (kN)	Friction pressure (MPa)	Burn-off length (mm)	Rot. speed (U/min)	Forge force (kN)	Forge pressure (MPa)	Forge/holding time (s)
S355-S355	0.5	25.1	80	6	1900	50.3	160	5
S355-1.4301	0.5	20.7	80	6	1900	56.9	181	5

Fig. 5 Exemplary process graph for welded S355-S355 specimen

method. For connections with flash, the flash has been mechanically removed to provide access for the measurement. The measurements were performed along a line in the axial direction of the specimens. The measurement interval was 1 mm, and the collimator opening diameter was 1.5 mm. For series S355-S355, low compressive residual stresses around $\sigma_{RS} = -30$ MPa are observed, owing to the stress relief treatment. Series 2 (S355−1.4301) shows compressive residual stresses up to $\sigma_{RS\perp} = -380$ MPa in axial resp. loading direction and $\sigma_{RS\parallel} = -180$ MPa in tangential direction close to the flash base notch.

The specimens without flash made from S355-S355 show, due to the stress relief treatment, low residual stresses in tangential and axial direction. However, at the specimens made from S355 and 1.4301, high compressive residual stresses are measured. These stresses are caused by the mechanical removal of the flash and the outer material layer of the specimen.

3.2 Microsections and hardness

Microsections have been prepared for both material combinations (Fig. 6).

A symmetric flash can be identified for the single-material joint. The joined net section at the interface has a largely increased diameter of $D_S = 25.8$ mm compared to the net section of the base materials. Accordingly, the flash fork notch is positioned in a location with low stresses.

For the dissimilar joint, the volume of the excess material that is displaced to the outside from the fusion zone is higher for the S355 compared to 1.4301 resulting in a non-symmetric fork. The overall net section at the interface of both materials ($D_S = 23.2$ mm) is larger compared to the net section of the shaft ($D_i = 20$ mm).

In addition, the hardness of the specimens was measured by UCI and indentation (Figs. 7 and 8). For both variants, an increase in hardness towards the interface could be deter-

mined. The stress relief heat treatment leads to a decrease in hardness of about 10% for the S355.

3.3 Local weld geometry

The radii of the flash base notches have been measured from the microsections and averaged. The radii at the series 1 specimens were uniformly determined to $r = 1.7$ mm. For the series 2 specimens, a radius of $r = 3.3$ mm was observed on the 1.4301 side, while the radius in the S355 was comparatively lower at $r = 0.5$ mm. In addition, some bulging can be observed in front of the radii, to which they are con-
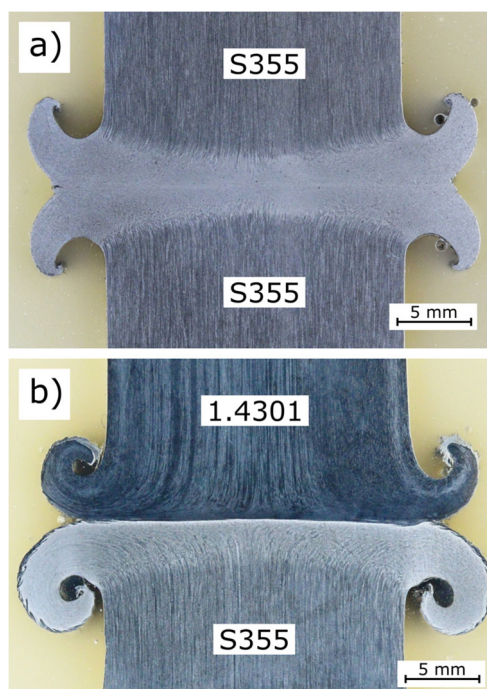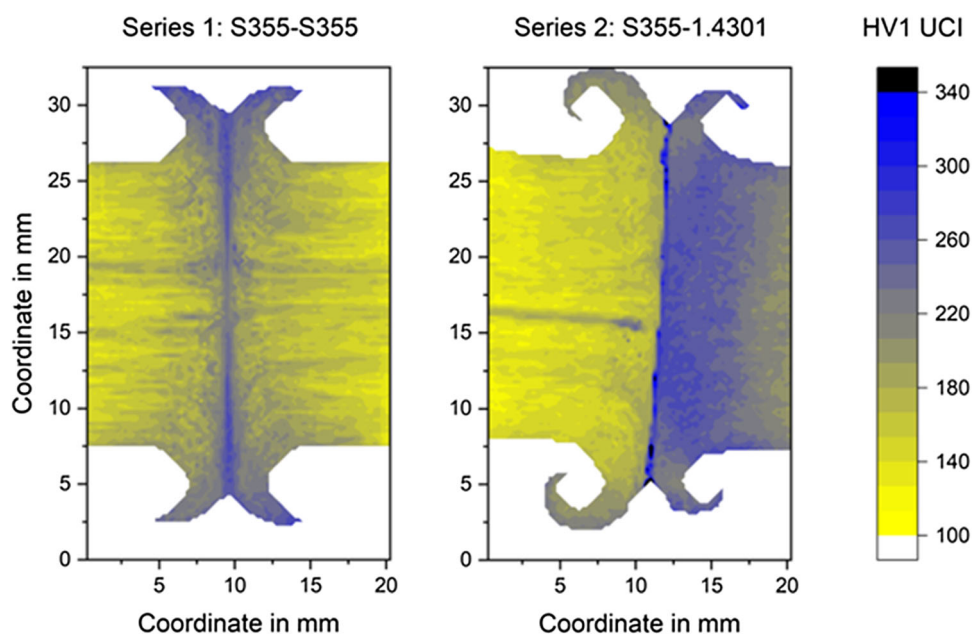

Fig. 6 Microsections of the specimens **a** S355-S355 with flash and **b** S355-1.4301 with flash

Fig. 7 UCI-hardness of the specimens **a** S355-S355 with flash and **b** S355-1.4301 with flash

4 Fatigue investigations

4.1 Fatigue tests

Fatigue tests of the rotary friction welded specimens were experimentally conducted in servo-hydraulic test rigs under constant amplitude loading and load control. Tests have been conducted under torsional and axial loading with $5\,\text{Hz} \leq f \leq 15\,\text{Hz}$. For all fatigue tests, the R ratio was set to $R = -1$.
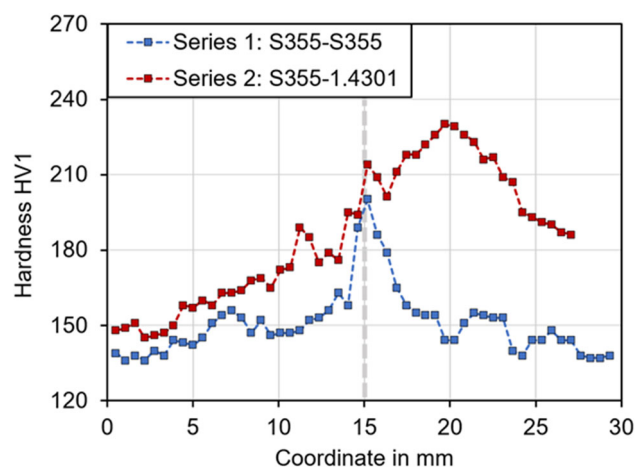

Fig. 8 Hardness HV1 of both specimens measured on a straight path at a distance of 0.5 mm from the surface

The fatigue tests on specimens with axial loading were conducted until the total fracture of the specimens. During all tests, the deflection amplitude and the mean deflection have been recorded. The testing in torsion was stopped at different stages of increased torsional angle while the angle was recorded for all tests. Testing had to be stopped before complete failure, since the specimens would otherwise be too severely deformed to observe crack locations. The failure criterion for torsional and axial loading was set to a reduction in stiffness by $\Delta\alpha = 5\%$.

As a result of the fatigue test, overall, eight S-N curves have been derived, each four for the dissimilar and single-material specimens with and without flash under axial loading and four under torsional loading (Figs. 9 and 10). For the statistical evaluation, the maximum likelihood approach according to [22] was applied. Since the S-N curves for every condition (axial and torsion loading, with and without flash) showed similar slopes and knee points, a joint evaluation was conducted.

For the axially loaded specimens with flash, a bi-linear S-N curve is identified. At cycles $N_{k,1} \leq 2 \cdot 10^5$, a shallower slope of $m_1 = 12$ is identified whereas the slope at $N_{k,1} \geq 2 \cdot 10^5$ of $m_2 = 6.5$ is much steeper. The position of the knee point towards a higher number of cycles was determined at $N_{k,2} \geq 2 \cdot 10^6$. The dissimilar joint reaches with $\Delta\sigma_{n,2e6} = 349\,\text{MPa}$ an approx. 8% higher fatigue strength than the single-material joints with $\Delta\sigma_{n,2e6} = 323\,\text{MPa}$.

The axially loaded specimens with flash removed show an overall higher fatigue strength than the specimens with flash at $N > 2 \cdot 10^4$ cycles. The S-N curve has a slope of $m = 18$ independent of the material combination. However, the dissimilar joints have an approx. 10% higher fatigue
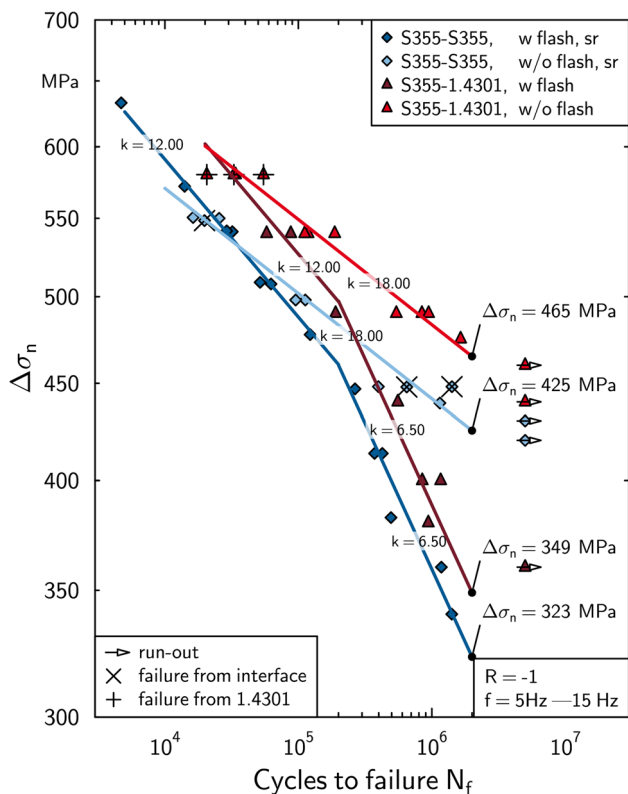
Fig. 9 Fatigue test results for friction welded joints under axial load

Fig. 10 Fatigue test results for friction welded joints under torsional load with and without flash

strength of $\Delta\sigma_{n,2e6} = 465$ MPa compared to the single-material joints with $\Delta\sigma_{n,2e6} = 425$ MPa. In contrast to the specimens with flash, no second kink in the S-N curve can be observed towards higher cycles.

The S-N curves of the specimens with flash under torsional loading have a slope of $k = 15$. An approx. 10% higher fatigue strength of the dissimilar welded specimens ($\Delta\tau_{n,2e6} = 345$ MPa) can be observed compared to the single-material ones ($\Delta\tau_{n,2e6} = 315$ MPa). As for the specimens with the flash removed under torsional loading, a slope of $k = 18$ was observed. The fatigue strength at $N = 2 \cdot 10^6$ was slightly improved.

4.2 Failure behaviour and fractography

For all specimens with flash under axial fatigue load, failure initiates at the flash base notch of the material S355. The cracks initiate at one or several positions at the circumference and grow through the base material. The specimens with flash removed failed in the majority of cases in the base material S355 at the transition between the net section and transition radius, away from the heat affected zone. Only two specimens failed from the centre of the interface; however, these did not show a significantly lower fatigue life (Fig. 9).

For the specimens with flash tested using a torsional fatigue load, fatigue cracks were initiated at the flash base
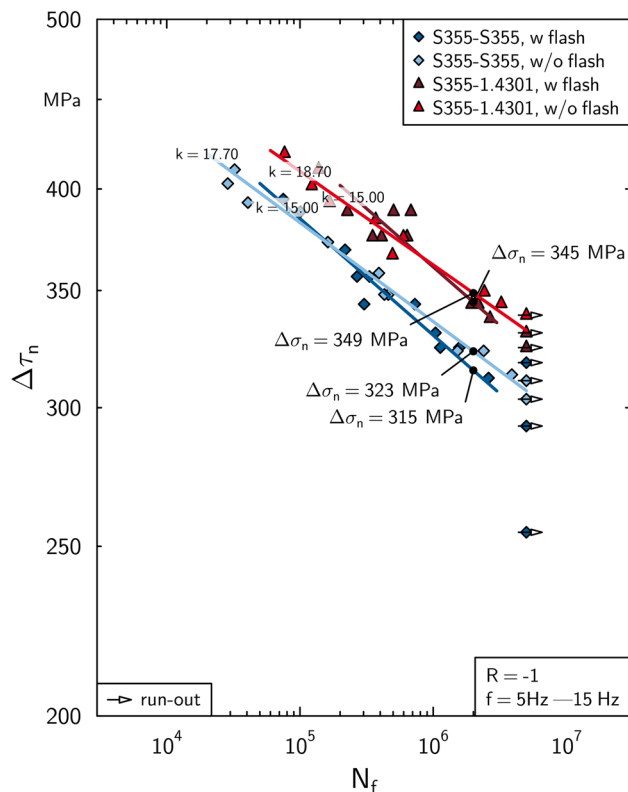
notch or the base metal of the S355 (Fig. 11). Cracks often occurred at multiple locations around the circumference and grew either in longitudinal, circumferential or 45° directions. At lower load levels, one major crack tended to dominate the fatigue behaviour, while at higher loads, multiple cracks were initiated. Of the stress relieved series 1 specimens, nine failed from the flash base notch and two from the base metal S355. In series 2, failure occurred always in the S355, three times from the flash base notch and six times from the base metal. For all torsion specimens with the flash removed, the failure occurred in the base metal S355 (Fig. 12).

5 Discussion

For conventionally GMAW-welded butt joints with high quality (small weld reinforcement, low amount of misalignment), an endurable fatigue strength of $\Delta\sigma = 90$ MPa (FAT 90) is recommended for axial loading [16] (Fig. 13). The slope of the design S-N curve is set to $k = 3$, the knee-point positioned at $N_k = 10^7$ cycles and the survival probability is $P_S = 97.7\%$. Compared to these recommendations, the fatigue tests on the specimens with flash $\Delta\tau_n = 315$ MPa and $\Delta\tau_n = 345$ MPa show a much high fatigue strength. This is also true if the results are compared to fatigue data

Fig. 11 Fatigue crack initiation at a specimen with flash under torsional loading starting from the surface of the base material

for butt welds with a double-V weld ($P_S = 50\%$) taken from an S-N catalogue [23].

These substantially higher fatigue resistance can be explained by various reasons:

1. In contrast to the conventionally welded joints, the radii in the fatigue-critical regions, i.e. the flash base notch, of the friction welded joints are much larger. These larger radii lead to an increase in fatigue strength and a shallower slope [15, 24, 25] of the S-N curve. It is important to mention that the increase in fatigue strength is also caused by the increase in diameter D_S of the weld interface. This increase in diameter decreases the nominal and local stress at the flash fork notch which has geometrical features of conventionally welded joints—sharp, crack-like. In case of a much smaller diameter at the interface, i.e. $D_S \leq D_i$, a strong decrease in fatigue strength is
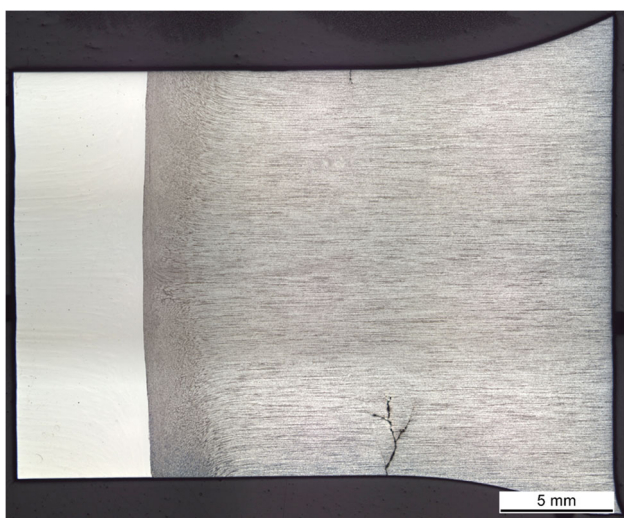

Fig. 12 Fatigue crack initiation at a specimen without flash under torsional loading starting from the surface of the base material
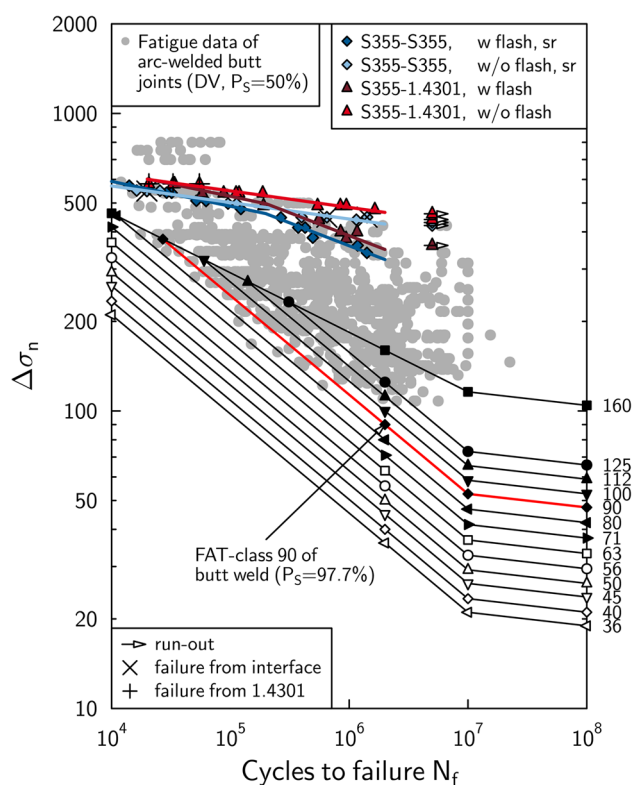

Fig. 13 Fatigue test results for friction welded joints under axial load ($R = -1$, $P_S = 50\%$ compared to the design recommendation from [16] ($R = 0.5$, $P_S = 97.7\%$) and literature data for butt joints with double-V weld [23]

expected; however, this could not be observed experimentally in this work.

2. The presence of high tensile residual stresses for conventionally GMAW-welded joints or complex structures is an assumption in all major rules and guidelines for the assessment of welded joints. This approach might not necessarily be adopted for friction welded joints. At least in the specimens under investigation and in [26], compressive residual stresses were measured close to the flash base notch. In order to give any generalized recommendations, a much higher variety of welded joints with different materials and geometrical configurations need to be investigated. Conversely, this means that a mean stress sensitivity should be considered in the fatigue assessment if mean stresses higher than zero are present.

3. The fatigue tests in these investigations have been conducted at zero mean stress, i.e. an R ratio of $R = -1$. This, in connection with the high compressive residual stresses, leads to an increase in fatigue strength. Under consideration of a mean stress sensitivity of $M = 0.33$ as in the IIW-recommendations, a factor of $f = 1.6$ between the endurable stresses at $R = 0.5$ and $R = -1$ may be assumed [16].

4. Finally, the design S-N curves are developed, derived and defined for a survival probability of $P_S = 97.7\%$. This needs to be considered when comparing individual fatigue tests with design S-N curves.

If the influence of mean stresses resp. residual stress (factor $f = 1.6$) and survival probability (factor $f = 1.37$; if a scatter of $T_S = 1 : 1.5$ is assumed) is considered, still, a large difference between the experimental data 350 MPa/1.6/1.37= 160 MPa and the design values $\Delta\sigma = 90$ MPa (FAT90) can be observed. This shows the high potential of friction welded joints in terms of their fatigue behaviour, especially for high-cycle applications because of the comparatively shallow slope in the high-cycle fatigue regime. A removal of the flash leads to an even higher fatigue strength.

As for the welded joints under axial loading, the same effects apply for the specimens under torsional loading. Here, the characteristic fatigue strength of $\Delta\tau_n = 315$ MPa is factor $f > 3$ higher than the endurable stress of $\Delta\tau_n = 100$ MPa recommended [16]. The flash exerts little influence on the fatigue strength under torsional loading

In case of the absence of sharp notches, an influence of the base material strength on the fatigue strength may be assumed [27]. This should lead to the possibility to further increase the fatigue strength and fully exploit the lightweight potential of welded joints. However, in any case, a high weld quality, i.e. the absence of sharp notches and other irregularities, needs to be assured by a process control and a subsequent quality assurance.

For a fatigue assessment, the following approach seems to be applicable: First, the fatigue strength of the base material at the flash base notch needs to be assessed. It is recommended to use the FKM-guideline [17], since the governing parameters, such as materials strength, stress gradients and surface roughness, can be assessed. Second, an assessment of any sharp-like notches, such as the flash fork notch, needs to be performed. This can be conducted with a reference radius ($r_{ref} = 1$ mm or $r_{ref} = 0.05$ mm) typically used for the fatigue assessment of welded joints. Since no failure was achieved at this location in the investigations, these theoretical assumptions need to be validated in future research.

In any case, the shape of the flash is expected to have a significant influence on the fatigue strength. A large radius of the flash base notch is favourable to achieve a high fatigue strength. Additionally, the diameter of the net section at the interface should be higher than the one in the net section at the base material, to reduce the nominal stress and the risk of cracks initiating from the flash for notch. A finite element analysis of the specimens resulted in stress concentration factors under axial loading in the range $1.7 \leq K_{t,\sigma} \leq 1.9$ (S355), $K_{t,\sigma} \approx 1.4$ (1.4301) that are comparatively higher than the ones under torsional loading: $1.2 \leq K_{t,\sigma} \leq 1.35$

(S355), $K_{t,\sigma} \approx 1.15$ (1.4301). The lower stress concentration under shear loading becomes visible at high cycles, where there is a much higher difference in fatigue strength between specimens with and without flash under axial loading compared to torsional loading.

Further, fatigue tests and numerical evaluations should be conducted, to validate the proposed approach.

6 Conclusion

From the investigations performed, the following main conclusions can be drawn:

- The metallurgical notch between the two materials did not lower the fatigue strength. At nearly all specimens, the failure under cyclic loading occurred outside the interface, i.e. the connection area of both materials.
- The sharp flash fork notch did not lower fatigue strength, likely due to being located outside of the load path in a region of increased cross sectional area.
- A highly increased fatigue strength of the friction welded joints compared to joints made by GMAW-processes could be identified. This increase can be explained by the absence of sharp notches. In addition, compressive residual stresses are present at the specimens made from S355-1.4301 due to machining and the friction welding process. These additionally increase the fatigue strength. A further increase in fatigue strength with increasing static strength of the base material might be expected.

Declarations

Conflict of interest The authors declare no competing interests.

References

1. ISO 15620:2019: Welding - friction welding of metallic materials. Int Organ Standard
2. Merkblatt DVS2909, Teil 1: Reibschweißen von Metallischen Werkstoffen - Rotationsreibschweißen: Verfahren, Begriffe, Werkstoffe (engl.: Code of Practice DVS2909, Part 1: Friction Welding of Metallic Materials - Rotary Friction Welding: Processes, Terms, Materials). DVS - Deutscher Verband für Schweißen und verwandte Verfahren e.V
3. Brutscher T (2003) Reibschweißen von Gelenkwellen für PKW und kleine Nutzfahrzeuge (engl.: Friction welding of drive shafts for passenger cars and small commercial vehicles). In: 13. Erfahrungsaustausch Reibschweißen der SLV München GmbH
4. Dzhabarov RD, Fataliev NS, Tkachev YA, Timofeev VI, Abdullaev VG (1994) Application of friction welding in petroleum and chemical engineering. Chem Pet Eng 30(9):451–455
5. Schnabel W (2006) Reibschweißen von Verankerungen im Brückenbau (engl.: Friction welding of anchorages in bridge construction). Geesthachter Schweißtage 2006:47–54
6. Baxter GJ, Preuss M, Withers PJ (2002) Inertia friction welding of nickel base superalloys for aerospace applications. In: International Conference on Microstructure and Performance of High-temperature Alloys
7. Weiß R (1994) Festigkeit und Eigenspannung reibgeschweißter Keramik-Metallverbunde (engl.: Strength and residual stress of friction-welded ceramic-metal composites). Technical report, Deutscher Verband für Schweißen und verwandte Verfahren (DVS)
8. Ponesakki Raja P, Bensam Raj J (2017) Investigations on mechanical and metallurgical properties of friction welding of AlB2 reinforced aluminum matrix composites. Silicon 10(4):1385–1391. https://doi.org/10.1007/s12633-017-9615-0
9. Na S-J (1993) Das Reibschweißen ungleichartiger Metalle (engl.: friction welding of dissimilar metals). PhD thesis, Technische Universität Braunschweig
10. Nentwig AWE (1986) Reibschweißen Von Wolfram (engl.: Friction Welding of Tungsten), p. 189. Deutscher Verlag für Schweißtechnik, Düsseldorf
11. Nu HTM, Le TT, Minh LP, Loc NH (2019) A study on rotary friction welding of titanium alloy (Ti6Al4V). Adv Mater Sci Eng 2019:1–9. https://doi.org/10.1155/2019/4728213
12. Neumann A, Schober D (1990) Reibschweißen von Metallen; Konstruktion Technologie Qualitätssicherung (engl.: Friction Welding of Metals; Design, Technology and Quality Assurance). Deutscher Verlag für Schweißtechnik; DVS-Verlag GmbH, Düsseldorf
13. Wang G, Li J, Xiong J, Zhou W, Zhang F (2018) Study on microstructure evolution of AISI 304 stainless steel joined by rotary friction welding. Welding in the World 62(6):1187–1193. https://doi.org/10.1007/s40194-018-0613-7
14. Radaj D, Sonsino CM, Fricke W (2006) Fatigue assessment of welded joints by local approaches. Woodhead Publishing Limited, Cambridge. https://doi.org/10.1533/9781845691882
15. Braun M, Fischer C, Baumgartner J, Hecht M, Varfolomeev I (2022) Fatigue crack initiation and propagation relation at notched specimens with welded joints characteristics. Metals 12(4):615. https://doi.org/10.3390/met12040615
16. Hobbacher AF (2016) Recommendations for fatigue design of welded joints and components. Springer, Switzerland. https://doi.org/10.1007/978-3-319-23757-2
17. Rennert R, Kullig E, Vormwald M, Esderts A, Luke M (2020) FKM guideline - analytical strength assessment of components, Forschungskuratorium Maschinenbau (FKM)
18. Hasegawa M, Ieda T, Taki N (1997) Fatigue strength of friction welded joints of various carbon steels with flash. Q J Japan Weld Soc 15(1):115–121. https://doi.org/10.2207/qjjws.15.115
19. Paventhan R, Lakshminarayanan PR, Balasubramanian V (2011) Fatigue behaviour of friction welded medium carbon steel and austenitic stainless steel dissimilar joints. Mater Des 32(4):1888–1894. https://doi.org/10.1016/j.matdes.2010.12.011
20. Neumann A, Schober D (1994) Bewertungsgruppen von Reibschweißverbindungen und deren Berechnung bei statischer und schwingender Beanspruchung (engl.: Quality levels of friction welded joints and their calculation under static and cyclic loading). In: Große Schweißtechnische Tagung, pp 173–178
21. DDR-Standard TGL 19340/03: Ermüdungsfestigkeit, Dauerfestigkeit der Maschinenbauteile, Berechnung (engl.: GDR standard TGL 19340/03: Fatigue strength, fatigue strength of machine components, calculation). Verlag für Standardisierung (March 1983)
22. Störzel K, Baumgartner J (2021) Statistical evaluation of fatigue tests using maximum likelihood. Materials Testing 63(8):714–720. https://doi.org/10.1515/mt-2020-0116
23. Olivier R, Ritter W (1979) Wöhlerlinienkatalog Für Schweißverbindungen aus Baustählen - Teil 1: Stumpfstoß (engl.: S-N Catalogue for Welded Joints - Part 1: Butt Joints). Deutscher Verlag für Schweißtechnik (DVS) GmbH, Düsseldorf
24. Hück M, Thrainer L, Schütz W (1983) Berechnung von Wöhlerlinien für Bauteile aus Stahl, Stahlguß und Grauguß - Synthetische Wöhlerlinien (engl.: Calculation of Wöhler curves for components made of steel, cast steel and grey cast iron - Synthetic Wöhler Curves). Technical report, Industrieanlagen-Betriebsgesellschaft mbH, Ottobrunn/München
25. Eichlseder W (2002) Fatigue analysis by local stress concept based on finite element results. Comput Struct 80:2109–2113
26. Manteghi S, Gibson D, Johnston C (2017) Fatigue performance of friction welds manufactured both in air and underwater. In: 36th International Conference on Ocean, Offshore & Arctic Engineering (OMAE2017). Am Soc Mech Eng, New York. https://doi.org/10.1115/OMAE2017-62495
27. Sonsino CM (2007) Light-weight design chances using high-strength steels. Mater Werkst 38(1):9–22. https://doi.org/10.1002/mawe.200600090